A study of the isotope shift in chromium
by Charles Albert Lincoln

A thesis submitted to the Graduate Faculty in partial fulfillment of the requirements for the degree of
MASTER OF SCIENCE in Physics
Montana State University

Abstract:
The isotope shift in chromium was measured using Fabry-Perot interferometric technique. The shift was observed in the 5D4.-5P3 line and in the 5D1-5P1 line for the atomic numbers 50-52. The normal mass effect and the volume effect were calculated and compared to the observed shift. The resulting residual shift was attributed to the specific mass effect. No attempt was made to calculate the specific mass effect theoretically.

The experimentally observed shift was 85±5 mK. The volume effect shift was calculated to be 4 mK. The normal mass effect was calculated to be 7.7 mK. The residual shift was then 81±5 mK.

A three prism Steinheil-Streander spectrograph with a Fabry-Perot interferometer was used. A hollow cathode discharge tube (cooled in liquid air) with chromium trioxide on the surface of the hollow cathode comprised the remaining important features of the experimental set-up.

A STUDY OF THE ISOTOPE SHIFT IN CHROMIUM

by

CHARLES ALBERT LINCOLN

A thesis submitted to the Graduate Faculty in partial fulfillment of the requirements for the degree

of

MASTER OF SCIENCE

in

Physics

Approved:

Irving C Dayton
Head, Major Department

Roy V. Kriegsmann
Chairman, Examining Committee

Louis D. Smith
Dean, Graduate Division

MONTANA STATE COLLEGE
Bozeman, Montana

June, 1964

ACKNOWLEDGMENT

This Thesis represents the extension of some work done by Dr. Hack Arroe. It was largely by means of his patience and understanding help that the thesis was completed. Dr. Roy Wiegand took much of his time in constructive criticism and made many useful remarks. Drs. Joseph Ball and E. Miller Layton also read the thesis and offered constructive criticism.

The author is extremely thankful to the above-mentioned individuals for their help. Also, thanks are due to Mrs. Harlan Wilhelm for the excellent typing.

A special word of thanks is given to the author's wife for her much-appreciated encouragement.

TABLE OF CONTENTS

LIST OF TABLES

LIST OF FIGURES

ABSTRACT

The isotope shift in chromium was measured using Fabry-Perot interferometric technique. The shift was observed in the $^5D_4$-$^5P_3$ line and in the $^5D_1$-$^5P_1$ line for the atomic numbers 50-52. The normal mass effect and the volume effect were calculated and compared to the observed shift. The resulting residual shift was attributed to the specific mass effect. No attempt was made to calculate the specific mass effect theoretically.

The experimentally observed shift was 85 ± 5 mK. The volume effect shift was calculated to be 4 mK. The normal mass effect was calculated to be 7.7 mK. The residual shift was then 81 ± 5 mK.

A three prism Steinheil-Streander spectrograph with a Fabry-Perot interferometer was used. A hollow cathode discharge tube (cooled in liquid air) with chromium trioxide on the surface of the hollow cathode comprised the remaining important features of the experimental set-up.

INTRODUCTION

Optical spectroscopy has been the major tool in the analysis of atomic structure.[1] With the advent of high resolution spectroscopy, first used by Michelson in 1892,[2] and the development of a theory to explain the hyperfine structure of the multiplet lines in the atomic spectra which were subsequently observed, optical spectroscopy has become an important tool in the analysis of nuclear structure.[3] In 1924, Pauli[4] proposed that the hyperfine structure (HFS) results from a magnetic coupling between the nucleus and its orbital electrons. Pauli's explanation was soon shown to be essentially correct, but some HFS experiments yielded anomalous values. These anomalies were later interpreted as due to an effect called isotope shift. This paper contains a brief review of the theories dealing with the HFS and with isotope shift. Since isotope shift and HFS utilize similar assumptions on the nucleus, both are treated here.

In the Bohr theory of the atom,[5] the nucleus is assumed to be a point charge, and the interaction between the nucleus and the electrons is a coulomb type. This simple assumption is useful as a first approximation and serves to describe the gross structure of the atom. The intrinsic spin and magnetic

moment of the electron is required for an explanation of the observed fine structure in atomic spectra. If it is also assumed that the nucleons have an intrinsic spin and that the nucleus has a resultant angular momentum and magnetic moment, then the HFS can be related to the resulting interactions between the magnetic multipole moments of the nucleus and the electrons.

The energy levels contributing to the production of HFS are due, in general, to the magnetic interaction mentioned above. However, the levels may be modified by the addition of a factor, which is usually small, arising from an electrostatic interaction between the nucleus and the electrons. Some of the results from the analysis of fine structure apply to hyperfine structure since they arise from similar effects. Among these are the Lande interval rule,[3] and the selection rules.[3] HFS also exhibits Zeemann and Paschen-Back effects similar to those found in fine structure and are treated in a similar manner.[6] Experimentally, hyperfine structure is observed only if the nucleus has non-zero angular momentum. This condition is satisfied in atoms with odd-even, even-odd, and odd-odd nuclei. That is, with an odd number of protons and an even number of neutrons, etc.. Hyperfine structure

will be discussed more completely in part II.

The isotope shift studies fall naturally into two categories; the mass and the volume effects. The mass effect is further divided into the normal and specific mass effects. These effects are described in part III. The volume effect has many aspects and gives much insight into the structure of the nucleus. The experimental data on the volume effect would indicate that the term shift is caused mainly by s electrons, the sign of the shift being obtained by assuming that the s electron raises the level of the heavier isotope relative to the lighter one. Experiments also show that the spectral lines of the even isotopes are always arranged in the order of their mass numbers, and separations tend to be of the same order of magnitude for different isotopes in a particular spectral line. Odd-even staggering is observed i.e. the lines of the odd isotopes are shifted towards the isotope of lower atomic number. These features are shown graphically in Fig. 1. Mack and Arroe[7] have written an excellent review which includes a survey of the literature of the isotope shift studies to 1956. The volume effect will be discussed more completely in part IV.

The following explanation of figure 1 is taken from

the review article by Mack and Arroe;[7] "Figure 1a shows a term shrinkage that occurs in all spectra, and is the only shift in the spectra in the hydrogen-like isoelectronic sequence: the shift (measured from the value postulated for an infinitely massive nucleus) tends to reduce the term differences and is strictly proportional to the term value and to the reciprocal of the mass of the atom or ion; thus the separation between adjacent mass numbers is approximately inversely proportional to the square of the average mass. This universal term shrinkage is completely accounted for as the normal mass effect. For simplicity it is not shown in the other parts of figure 1, all of which show selective shifts, i.e., shifts occurring only in certain levels.

"In its simplest manifestation (Fig. 1b), from Z=2 through about the first third of the atomic table, the selective shift of a level may be either sign, depending on the electron quantum numbers; and the magnitude of the shift per unit mass change for those levels that are most strongly affected in any spectrum is somewhat smaller than the normal mass effect and varies from element to element in roughly the same way, i.e., inversely as the mass squared, or approximately linearly in the mass when the mass differences are

small compared with the mass itself. This shift is identified with the specific mass effect.

"All of the following phenomena are attributed to the field effect, and the usual hypothetical reference level is not that with infinite mass but that with zero volume (zero mass). About where the specific mass effect becomes inappreciable (10^{-3}K, where K stands for Kayser, or cm^{-1}) there begins to be noticeable, but only among certain levels (Fig. 1c), an increase in the energy with increasing mass. The energy change depends only upon the configuration, and is greatest in the case of a configuration with a single unbalanced s electron; but for a $p_{\frac{1}{2}}$-electron it grows to about one-fifth this magnitude in heavy atoms. Notice that the only characteristic distinctions to be observed experimentally between the specific mass effect (Fig. 1b) and the field effect when the latter is approximately linear (Fig. 1c) are that the former may have either sign while the latter is always negative; also, the two effects differ markedly with respect to their dependence upon the electronic quantum numbers.

"Figure 1d illustrates odd-even staggering (. . .).

"Figure 1e shows the most general situation, which is

beginning to be recognized as the usual one in the field effect region of the atomic table; even for increases of 2 in N (i.e., when N stays odd or stays even) the position of the level is appreciably nonlinear in N."

Fig. 1

General Features of Atomic Isotope Shifts

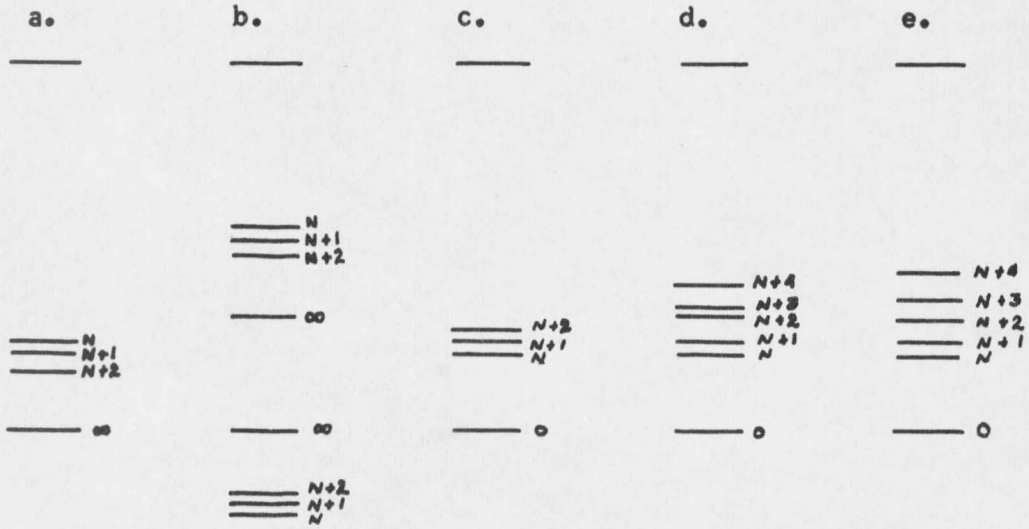

a. Normal Mass Effect

b. Specific Mass Effect

c. Linear Volume Effect

d. Odd-Even Staggering

e. General Volume Effect

II. HYPERFINE STRUCTURE

The following is a review of the magnetic and electrostatic interactions between a nucleus and the core electrons. The results are qualitatively the same as those obtained from a rigorous quantum mechanical treatment with only a few minor alterations. A more thorough treatment is to be found in the literature.[3]

A. Magnetic Dipole Interaction between Atomic Nucleus and Orbital Electrons

From classical electrodynamics, it is seen that the energy of magnetic interaction between an atomic nucleus and orbital electrons is given by[8]

$$U = -\int_V \vec{A}\cdot\vec{j}\, dv$$

where $\vec{A}$ is the nuclear vector potential, $\vec{j}$ is the current density of the electrons, and V indicates the volume of the atom. To a first approximation, the nucleus is considered a magnetic dipole and the vector potential is then given by,

$$\vec{A} = \vec{\mu} \times \vec{r} / r^3$$

where $\vec{\mu}$ is the magnetic moment of the nucleus. A better

approximation would be given by expanding $\vec{A}$ in powers of r^{-1}. This would resolve the nuclear magnetic field into monopole, dipole, quadrupole, and multipole components of higher order. However, poles of even order would not be symmetrical in the nucleus with respect to the nuclear equatorial plane, and, therefore, they cannot exist.* The magnetic octupole interaction contributes very little to the energy and there is no conclusive evidence that this interaction has been observed in optical spectroscopy. Neglecting terms higher than dipole, the interaction energy is written

$$U = -\int_v \frac{\vec{\mu}\times\vec{r}}{r^3}\cdot\vec{J}\,dv = -\int_v \vec{\mu}\cdot\frac{\vec{r}\times\vec{J}}{r^3}\,dv$$

The magnetic field of the electrons at the nucleus is[9]

$$H(0) = \int_v \frac{\vec{r}\times\vec{J}}{r^3}\,dv$$

The expression for the energy may be simplified by utilizing the relationship between the magnetic moment μ_I and the nuclear spin $\vec{I}$, $\mu_I = \frac{e}{2M}\hbar\vec{I}g_I$ where g_I is the nuclear

---

*See H. Kopferman[3] page 5. In particular; when the vector potential outside of the nucleus is expanded in powers of r^{-1}, then the first-order point source is the magnetic counterpart of the electric dipole. Second-order magnetic point sources correspond to the electric quadrupole.

gyromagnetic ratio and M is the proton mass. Using units of the nuclear magneton, $\mu_B \frac{m}{M} = \mu_m$, the relation is concisely written as

$$\mu_I = \frac{e}{2M} \hbar \vec{I} g_I \frac{m}{M} = \mu_B \vec{I} g_I \frac{m}{M}$$

which implies that

$$\frac{\mu_I}{\mu_m} = \vec{I} g_I$$

In order to obtain the shift of the energy levels, it is necessary to take the time average over the unperturbed electronic motion, that is:

$$\Delta W = -\mu_I \overline{H(0)} \cos(\vec{\mu}_I, \vec{H}(0)) ,$$

$\vec{H}(0)$ and $\vec{J}$ are anti-parallel for a single electron. The orbital angular momentum of the electron, $\vec{l}$, is directed opposite to the magnetic field that it produces at the nucleus, $\vec{H}_l(o)$. The intrinsic magnetic moment of the electron, $\vec{\mu}_s$, can be considered as being located on the electron orbit and increases or decreases the field $\vec{H}_l(o)$ depending on whether $\vec{s}$ and $\vec{l}$ are parallel or anti-parallel. When $\vec{H}(o)$ and $\vec{J}$ are anti-parallel and g_I is positive, μ_I is most stable when it is parallel to $\vec{H}(o)$, then cos(I,J) = -1. This means

that the change in energy level is

$$\Delta W = \Delta W_{IJ} = A_{IJ} \cos(\vec{I},\vec{J}) \quad .$$

$\vec{I}$ and $\vec{J}$ precess jointly about the total angular momentum of the atom, $\vec{F}$, so that

$$\cos(\vec{I},\vec{J}) = (F^2 - I^2 - J^2) / 2IJ \quad .$$

In the quantum mechanical treatment, $\vec{\mu}_I$ is replaced by the component along the z axis, μ_{I_z} and $\vec{H}(o)$ by $H_z(0)$, F^2, J^2, and I^2 are replaced by $F(F+1)$, $J(J+1)$, and $I(I+1)$ respectively. $\vec{F}$ can take on all values $F = |I+J|, |I+J-1|, \ldots\ldots, |I-J|$. The change in energy levels is finally given by

$$\Delta W_{IJ} = A/2 \left[F(F+1) - I(I+1) - J(J+1) \right]$$

with

$$A = \mu_I \overline{H(0)} / IJ = \mu_n g_I \overline{H(0)} / J \quad .$$

B. Electrostatic Quadrupole Interaction between Nucleus and Orbital Electrons

The difference between the electrostatic interaction energies for a nucleus with finite volume and one of point

charge is

$$\Delta U = e\int_v \rho_m \varphi_e \, dv - Ze^2 \int_v \frac{\rho_e}{r} \, dv$$

where $e\rho_m$ is the charge density of the nucleus, $e\rho_e$ the charge density of the electrons and φ_e is the electrostatic potential of the orbital electrons. For electrons with zero charge density at the center of gravity of the nuclear charge, φ_e may be expanded in powers of (x,y,z) about the origin which is taken as the center of gravity of the nuclear charge. This gives, using an ordinary Taylor series expansion in three variables where, for example $\varphi_z = \frac{\partial \varphi}{\partial z}$ etc. an energy of

$$\Delta U = e\int_v \rho_m \varphi_e(0) dv + e\int_v \rho_m [x\varphi_x(0) + \cdots + z\varphi_z(0)] dv$$

$$+ e/2 \int_v \rho_m [x^2 \varphi_{xx}(0) + xy\varphi_{xy}(0) + \cdots] dv - Ze^2 \int_v \frac{\rho_e}{r} dv .$$

But $\varphi(0) = \frac{Ze}{r}$ and $\rho_m x$ corresponds to an electric dipole which vanishes in the nucleus from symmetry considerations. Thus the energy shift may be simplified to

$$\Delta U = 1/2 [\varphi_{xx}(0) e\int_v \rho_m x^2 dv + \varphi_{xy}(0) e\int_v \rho_m xy dv + \cdots + \varphi_{zz}(0) e\int_v \rho_m z^2 dv].$$

This is merely the double scalar product of two second rank

tensors Q_{ij} and φ_{ij} where

$$Q_{ij} = \int_v \rho_m x_i x_j \, dv \quad .$$

Transforming to a coordinate system with (ξ, η, ζ) specifically for the representation of the nuclear charge distribution and (x,y,z) for the electrostatic field, with symmetry about ζ and z respectively, the change of potential becomes

$$\Delta U_Q = e/2 \left[Q_{xx} \varphi_{xx} + Q_{yy} \varphi_{yy} + Q_{zz} \varphi_{zz} \right] \quad .$$

Note that from the cylindrical symmetry about the z axis and the fact that at the nucleus, $\nabla^2 \varphi = 0$ and $\varphi_{zz} = -2\varphi_{xx} = -2\varphi_{yy}$ that ΔU_Q may be written as

$$\Delta U_Q = \varphi_{zz} \, e/4 \int_v (3z^2 - r^2) \rho_m \, dv$$

and also that

$$\int_v (3z^2 - r^2) \rho_m \, dv = \int_v (3\zeta^2 - r^2) \rho_m \, dv \left(\tfrac{3}{2} \cos^2 \Omega - \tfrac{1}{2} \right)$$

where Ω is the angle between ζ and z. The expression,

$$e \int_v (3\zeta^2 - r^2) \rho_m \, dv \quad ,$$

is called the quadrupole moment.

The shift in energy level may be found by averaging over all of the unperturbed eigenvalues. (It must be kept in mind that this treatment is suitable only for cylindrically symmetric charge distributions, not for spherically symmetric distributions whose quadrupole moments are zero.) Thus ΔW_Q is given as

$$\Delta W_Q = e/4\ Q\ \overline{\varphi_{zz}(0)}\ \left(\tfrac{3}{2}\cos^2\theta - \tfrac{1}{2}\right) = B/4\left[\tfrac{3}{2}\cos^2(I,J) - \tfrac{1}{2}\right]$$

where

$$B = e\ Q\ \overline{\varphi_{JJ}(0)}\ ,$$

in the limit of large quantum numbers. Casimir[10] has shown that

$$\left[\tfrac{3}{2}\cos^2(I,J) - \tfrac{1}{2}\right] = \tfrac{3}{2}\left[C(C+1) - 2I(I+1)J(J+1)\right] / IJ(2J-1)(2I-1)$$

for small quantum numbers, where C is determined by

$$C = F(F+1) - I(I+1) - J(J+1)\ .$$

C. Determination of HFS Splittings

The total energy of a given level with quantum number F

may be represented by

$$W_F = W_J + AC/2 + B/4 \frac{3/2\, C(C+1) - 2IJ(I+1)(J+1)}{IJ(2J-1)(2I-1)} .$$

The separation (in wave numbers) between any pair of levels (1,2) is given as σ_{12} ,

$$\sigma_{12} = \frac{1}{2} A(C_1 - C_2) + \frac{3}{8} B\left[C_1(C_1+1) - C_2(C_2+1)\right] / I(2I-1)J(2J-1) .$$

Thus A and B may be determined from any two unperturbed intervals,[11] although more intervals may be used as a check on accuracy. When B is negligible the splitting of the levels is given by $W_F = W_J + AC/2$ and the total width of the splitting is given by

$$\Delta W = AI(2J+1) \text{ for } J \geq I , \quad \Delta W = AJ(2I+1) \text{ for } I \geq J ,$$

where ΔW is the interval from $|J+I|$ to $|J-I|$. The interval rule, however, always holds for HFS term differences. The intervals are in the ratio (I+J):(I+J-1):(I+J-2): etc..

D. Determination of μ_s from A

It is desirable, in many cases, to know the value of the nuclear magnetic moment. This may be found from the A values in HFS splitting. The change in energy level is regarded as

the sum of the change in energy level from the orbital magnetic field and from the spin magnetic field, that is

$$\Delta W_{IJ} = \Delta W_{Il} + \Delta W_{Is} \quad .$$

Using a treatment similar to that part A above the respective magnetic interactions are written

$$\Delta W_{Il} = -\mu_I H_l(0) \cos(\mu_I, H_l(0)) = -\mu_I H_l(0) \cos(I,l) \quad .$$

However,

$$H_l(0) = e \frac{(\vec{r} \times \vec{v})}{r^3}$$

and since angular momentum is quantized, $m(\vec{r} \times \vec{v}) = \vec{l}\,\hbar$, this implies that

$$\vec{H}_l(0) = \frac{e}{m} \hbar \frac{l}{r^3} \vec{l} \quad .$$

Regarding the electron and the nucleus as small magnets gives to a first approximation,

$$\Delta W_{Is} = \frac{\mu_I \mu_s}{r^3} \left[\cos(I,s) - 3\cos(I,r)\cos(r,s)\right] .$$

Combining these expressions, the resulting energy change is

$$\Delta W_{IJ} = \frac{1}{2} \left(\frac{e}{m} \hbar\right)^2 \frac{1}{r^3} g_I \left[I l \cos(I,l) - I s \cos(I,s) + 3 I s \cos(I,r)\cos(r,s)\right].$$

Goudsmit[17] has shown that this may be written as

$$\Delta W_{IJ} = A/2 \left[F(F+1) - I(I+1) - j(j+1) \right]$$

where

$$A = 2\mu_B^2 \frac{l(l+1)}{j(j+1)} \frac{1}{r^3} g_I \ .$$

Thus μ may be found from the HFS splitting factor.

III. THE MASS EFFECT IN ISOTOPE SHIFT[12,13,14]

The total kinetic energy of the atom is

$$T = -\sum_{i=2}^{n} \frac{\hbar^2}{2m_i} \nabla_i^2 \psi_e - \frac{\hbar^2}{2m_1} \nabla_1^2 \psi_n$$

in cartesian coordinates, where ψ_e is the electronic wave function, and the atomic particles are numbered from 1 to n where m_1 would for example represent the mass of the nucleus. To eliminate the nuclear motion, center of mass coordinates are introduced whereby the kinetic energy takes on the form

$$T = \left[-\frac{\hbar^2}{2m_1} \nabla_1^2 - \sum_{i=2}^{n} \frac{\hbar^2}{2m_i} \nabla_i^2 - \sum_{j \neq i} \frac{\hbar^2}{2m_i} \nabla_i \cdot \nabla_j \right] \psi_e \, .$$

The first term in this expression represents the center of mass motion and is disregarded. By introducing the reduced mass, the expression becomes

$$T = \left[-\frac{\hbar^2}{2m_r} \sum \nabla_i^2 - \frac{\hbar^2}{2m_i} \sum_{j \neq i} \nabla_i \cdot \nabla_j \right] \psi_e \, .$$

Here the first term causes the normal mass effect and the second term is the specific mass effect.

A. The Specific Mass Effect

The specific mass effect expresses the mutual coupling of electrons and hence does not occur in one electron atoms.

The energy of the coupling may be regarded as a perturbation, giving the additional energy

$$\Delta W = -\frac{\hbar^2}{2m_i} \sum_{i \neq j} \int_v \psi^* (\nabla_i \cdot \nabla_j) \psi \, dv \quad .$$

This may be integrated by parts, leading to a perturbation energy

$$\Delta W = -\frac{\hbar^2}{2m_i} \sum_{i \neq j} \int_v \nabla_i \psi \cdot \nabla_j \psi^* \, dv \quad .$$

Following Kopfermann,[3] a simple example is the two electron problem in a central potential. The zero order eigenfunctions, in terms of the eigenfunctions of the individual electrons u and v, are given by[11]

$$\psi = \frac{1}{\sqrt{2}} \left[u(1) v(2) \pm v(1) u(2) \right] \quad .$$

The plus sign holds for the singlet system and the minus sign for the triplet system. Inserting this into the expression for the energy reduces the energy expression to a single term

$$\Delta W = \frac{\hbar^2}{2m} \left| \int u^* \nabla v \, dv \right|^2$$

since

$$\int u^* \nabla u \, dv = 0 \quad .$$

But from the form of the electronic eigenfunctions, ΔW has a non-zero value only if $\Delta l = \pm 1$. Kopfermann[3] has given values for some configurations and their agreement with experiment.

B. The Normal Mass Effect

The Bohr theory of the atom adequately describes the normal mass effect for the hydrogen atom. For example the second line of the Balmer series shows a normal mass shift between H^1 and H^2 of 5.600 K,* in agreement with calculation. The deuterium component is on the high wave number side. The energy levels in terms of the reduced mass are

$$W_{m_p} = \frac{R_\infty Z^2}{n^2}\left(1 - \frac{m}{m_p}\right) = T_\infty\left(1 - \frac{m}{m_p}\right) .$$

This gives a line shift which is

$$\Delta\sigma \approx \frac{\sigma}{1836.12}\left(\frac{M_2 - M_1}{M_2 M_1}\right)$$

where M is the mass number of the nucleus, m_p the mass of the proton. It is easily seen that the normal mass shift is inversely proportional to M^2. For mass numbers on the order of 20 and larger, this effect is smaller than any observable HFS

---

*See the comments on figure 1.

splitting. Fig. 1 shows the main features of the normal and specific mass effects as well as the volume effect, which is treated in the following section. Fig. 2 shows graphically the normal mass effect as a function of the mass number as well as the line width due to the instrument and the line width due to Doppler broadening. The instrument line width and Doppler width are discussed in part V.

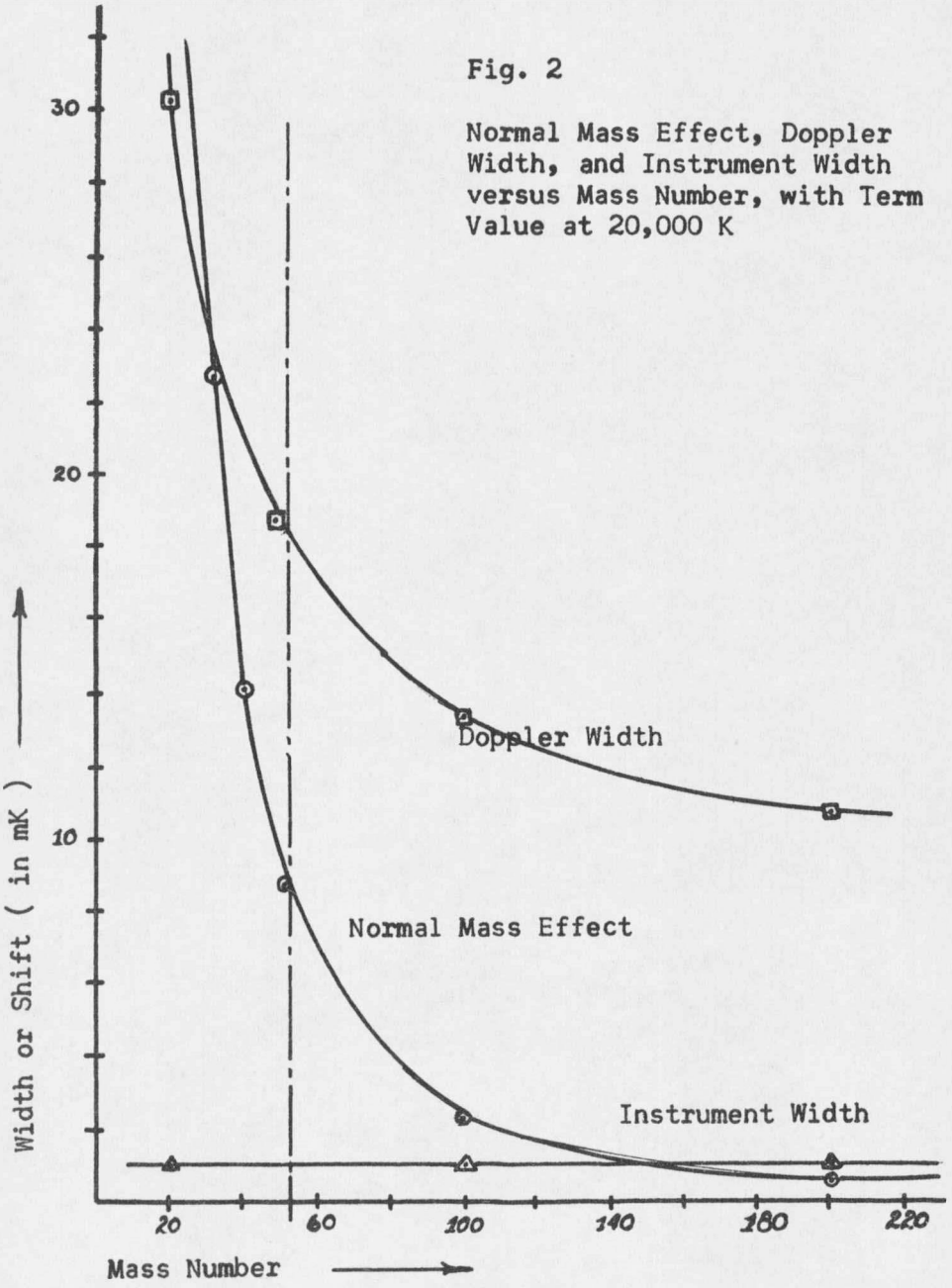

Fig. 2

Normal Mass Effect, Doppler Width, and Instrument Width versus Mass Number, with Term Value at 20,000 K

Doppler Width: $\Delta\sigma = \sigma (7.1) \times 10^{-7} \sqrt{\frac{T}{M}}$

Instrument Width: $\Delta\sigma = \frac{(1-\rho)\sqrt{1.5}}{2\pi d\sqrt{\rho}}$ 43

Normal Mass Effect: $\Delta\sigma = \frac{\sigma}{1836.12} \frac{M_1 - M_2}{M_1 M_2}$

IV. NUCLEAR VOLUME EFFECTS IN ISOTOPE SHIFT

A. Nuclear Charge Distribution

The initial work on a relativistic theory of the effects of finite nuclear size on the energy levels was done by Rosenthal and Breit[15] and Racah.[16] The perturbation method utilized by Rosenthal and Breit yields the following expression for the isotope shift of a single electron:

$$\Delta\delta W = \frac{4\pi R}{E} a_0^3 \psi^2(0) \frac{1+\rho}{[\Gamma(2\rho+1)]^2} y_0^{2\rho} \frac{\Delta y_0}{y_0} B$$

where:

$\psi^2(0)$ is the square of the non-relativistic atomic wave function at the center of the nucleus

a_0 is the radius of the first Bohr orbit

$\rho = (1 - Z^2\alpha^2)^{1/2}$, Z = nuclear charge; α = fine structure constant

$y_0 = 2Z r_0/a_0$, r_0 = radius of the nucleus

$\frac{\Delta y_0}{y_0}$ is the fractional change in nuclear radius with change in nuclear mass

B is a quantity dependent upon the charge distribution in the nucleus

The expression δW refers to the change in energy produced by the departure of the nuclear potential from the Coulomb potential of a point charge. The difference between the change in

energy of terms belonging to different isotopes of the same element is referred to as the differential shift, $\Delta\delta W$, and this is the shift which can be experimentally measured.

The theory is developed for s and p electrons, since only these electrons have an appreciable probability of being in the region of the nucleus.

Goudsmit,[18] Breit,[19] and Fermi and Segre[20] found the expression for $\psi^2(0)$,

$$\psi^2(0) = \frac{Z_i Z_a^3}{\pi a_o^3 n_o^3} \left(1 - \frac{d\sigma}{dn}\right)$$

where Z_i and Z_a are the effective nuclear charges in the inner and outer regions respectively, n_o is the effective principle quantum number, and σ is the quantum defect. For s electrons $Z_i = Z$. From the Bohr theory, the term value is

$$T = R Z_a^2 / n_o^2 .$$

This gives

$$\Delta\delta W = \frac{4 T^{3/2}}{Z_o R^{1/2}} \left(1 - \frac{d\sigma}{dn}\right) \frac{1+\rho}{\left[\Gamma(2\rho+1)\right]^2} y_o^{2\rho} \frac{\Delta y_o}{y_o} B .$$

Crawford and Schawlow[21] have calculated values of B for various charge distributions within the nucleus. Their results seem to indicate that a uniform charge distribution

yields values in closest agreement with experiment. The B value for a uniform charge distribution and a spherical nucleus is

$$B = \frac{3}{(2\rho+1)(2\rho+3)} \quad .$$

To find $(\Delta\psi_0)/\psi_0$ or, the same thing, $(\Delta r)/r$, the semi-empirical law for the nuclear volume[22] $r = r_0 M^{1/3}$, is used. This gives

$$(\Delta r)/r = (1/3)(\Delta M)/M$$

where M = mass number. Using this method and taking account of shielding effects (to be discussed later in part V), Brix and Kopferman[23] and Humbach[24] have analyzed a great deal of experimental data from many elements. The main results are briefly, (1) the observed shifts are on an average smaller by a factor of one-half than those predicted by the volume effect using $r_0 = 1.2 \times 10^{-13}$ cm; (2) the shifts vary with the neutron numbers in a manner which appears to be associated with the magic numbers,[24,25,26] (3) the odd-even staggering phenomena are still unexplained. These results (from the paper by Wilets, Hill, and Ford)[27] are shown in Fig. 3.

Fig. 3

Theoretical Curve and Experimental Points from Wilets, Hill and Ford[36]

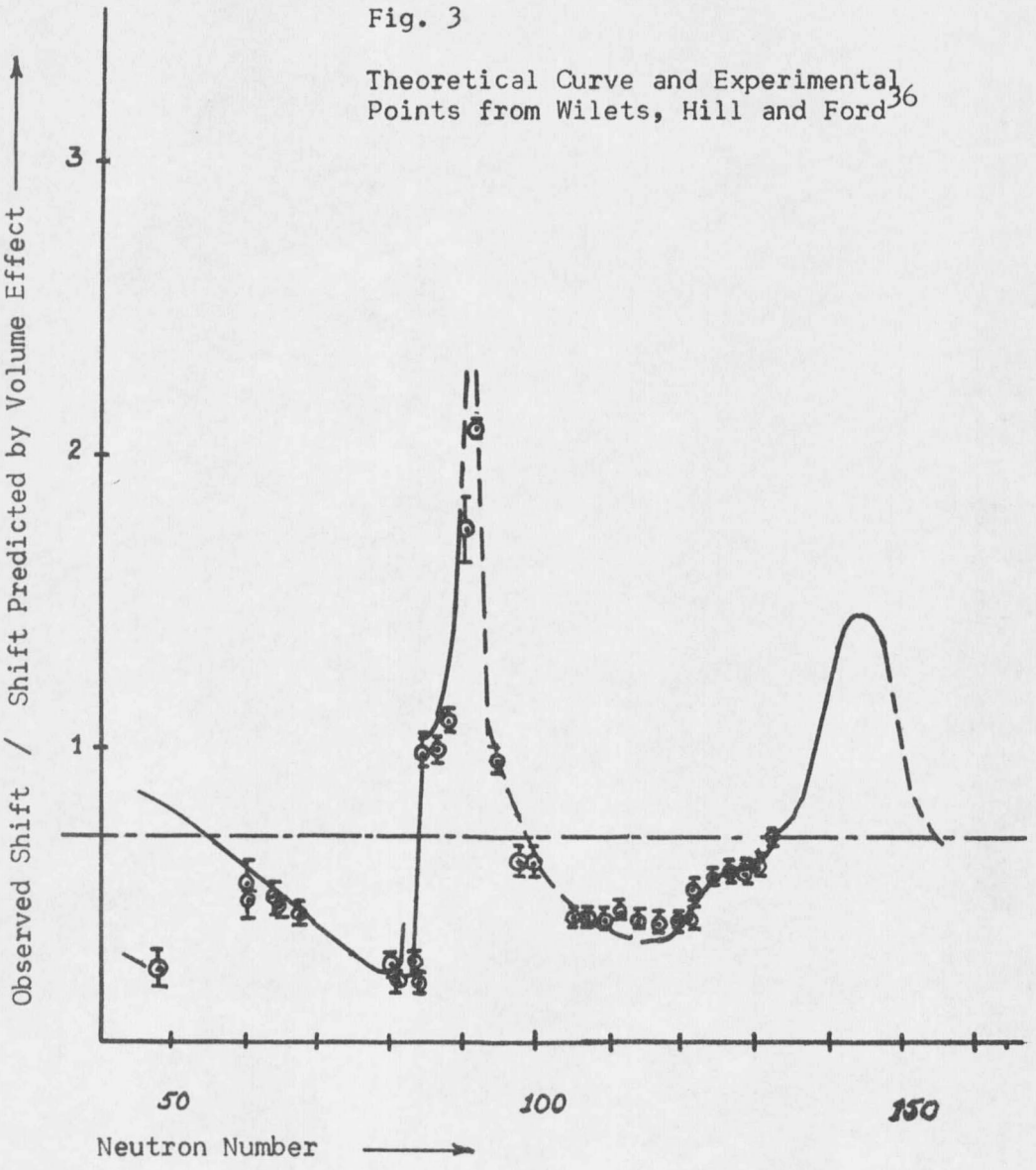

IV. B. Nuclear Deformation

Wilets, Hill, and Ford[27] have investigated some of the possible causes for the observed anomalies. Their investigations include studies of nuclear polarization, non-Coulomb forces, and distortion of the nucleus. They conclude that the distortion of the nucleus is the most probable cause of the anomalies.

The distortion of the nucleus is discussed in terms of nuclear models. The shell model with various coupling mechanisms[28] and the Bohr-Mottelson[29] unified model are two models that will be considered here. Wilets, Hill, and Ford have utilized the unified model in their paper and their results apply to this model.

The Shell Model

The shell model was first introduced as a means of explaining the existence of the "magic numbers."[30,31] An exact treatment of nuclear structure using inter-nuclear forces is not feasible, since the knowledge of these forces is limited. Moreover, those forces are so complicated that the mathematical difficulties of such a treatment are at present insurmountable. Thus the interaction of the individual nucleons with the remaining nucleons is described

by suitably chosen central fields of force within which they may move independently. An assumed over-all spherically symmetric potential accounts for the average effect of the attractions between nucleons. A square well potential is assumed for heavy nuclei and a parabolic potential well is assumed for light nuclei. These give rise to various energy levels and a coupling scheme is introduced so that the magic numbers correspond to the populations of filled energy levels.[3]

Rainwater's Model

The Bohr-Mottelson unified model is an extension of a model proposed by Rainwater.[31] In Rainwater's model, the nucleons in an incompletely filled subshell exert a centrifugal pressure on the "nuclear core" (filled shells, assumed rigid), causing it to be deformed to a shape with cylindrical symmetry. If the subshell is less than half filled with nucleons, a quadrupole moment is induced in a direction opposite to the nuclear spin. If the subshell is more than half full, the quadrupole moment is parallel to I but positive with respect to the normal quadrupole moment.

The Rainwater model, while it is a good approximation for weak deformations, is too crude to explain the differences

between the deformations of isotopes of an element.

Bohr-Mottelson Model

In the Bohr-Mottelson model the nuclear core is not regarded as a rigid sphere as in the Rainwater model, but is treated hydrodynamically as a liquid drop model. The nature of the nuclear fluid is such that the nucleus does not rotate as a rigid body but the rotations arise from circulating surface waves. The rotational energy, therefore, involves only the moment of inertia of that portion of the nuclear fluid that participates in the surface waves. Using this model as a basis, Bohr and Mottelson calculated the effective moment of inertia about an axis normal to the axis of symmetry of the volume. Their results show that the moment of inertia increases with increasing nuclear deformation regardless of the condition that the nuclear fluid motions be strictly irrotational. This model is the only workable one for strongly deformed nuclei.

2. Distortion of the Bohr-Mottelson Unified Model

Wilets, Hill, and Ford[27] have applied the Bohr-Mottelson model to the problem of the isotope shift anomalies. If the deformations are restricted to be cylindrically symmetric ellipsoidal, the nuclear radius is of the form

$$R(\theta) = a_0 [\, 1 + \alpha\, P_2 \cos\theta \,]$$

($\alpha > 0$ corresponds to prolate deformation, $\alpha < 0$ to oblate). Assuming a constant volume and a uniform charge density

$$\rho_0(r) = \frac{3 Z e}{4\pi a_0^3} \quad , \; r < R(\theta) \; ; \; \rho_0(r) = 0 \quad , \; r > R(\theta) \; ,$$

the constant volume assumption requires that

$$a_0 = a \left[\, 1 + (3/5)\alpha^2 + (2/35)\alpha^3 \,\right]^{-1/2} .$$

It must be kept in mind that α is the intrinsic nuclear deformation parameter and not the deformation measurable from quadrupole moments.[27] The perturbing energy of interest is the difference between the electron potential energy in the field of the deformed nucleus and that in the field of a spherical nucleus of the same charge and volume. Wilets, Hill, and Ford show that the ratio of the energy changes is

$$\frac{\Delta E_\alpha}{\Delta E_v} \doteq \frac{\rho (2\rho + 3)}{5} \alpha^2$$

where E_α corresponds to deformation energy and E_v corresponds to ordinary volume effect energy change and the ratio of the isotope shift from the deformation to the shift from the

volume effect is

$$\frac{\delta(\Delta E_\alpha)}{\delta(\Delta E_v)} = \frac{3}{10}(2\rho+3)A\left(\frac{\delta(\alpha^2)}{\delta N}\right)_z$$

The results of the work of Wilets, Hill, and Ford[27] provide an explanation for at least some of the anomalies observed in the heavier elements.

3. Nuclear Compressibility

The anomaly concerning the factor of one half in the ratio

$$\Delta\delta W_{experimental} / \Delta\delta W_{theoretical}$$

may be discussed in terms of the assumed constant in the semi-empirical law for the nuclear radius. By the most accurate results now available, the value of $r_o = 1.4 \times 10^{-13}$ cm used by Wilets, Hill, and Ford in their work is somewhat too large. A more reasonable value would be $r_o = 1.2 \times 10^{-13}$ cm.

Radii Determination

The semi-empirical formula $r = r_o M^{1/3}$ is only an approximation of the radius of the nucleus. Actually, the radius of the nucleus is not well defined since the density of nucleons is a quantum mechanical probability distribution. However, estimates of the radius which enclose most of the charge can

be made by several different experiments. The radius of the whole nucleus can be measured in some cases. Scott[32] has written a review article which covers the subject to 1955.

X-rays from mesic atoms[33]

The Bohr orbits of a negative μ meson near a nucleus are 210 times smaller than the electron orbits, since the μ meson is 210 times heavier than the electron. The size of the orbit in the lowest energy-level is of the same order as the size of the nucleus if the atom is at least moderately heavy. The energy of the ground state and of the K x-rays will then differ from those theoretically produced by a Coulomb charge because of the finite volume of the nucleus. The energy of these K x-rays depends quite sensitively on the radius of the nucleus. Fitch and Rainwater[34] observed the x-ray energies and deduced a value of $r_0 = 1.2 \times 10^{-13}$ cm. The detailed course of events when a μ^- meson is slowed to rest is very interesting.[32] After a few collisions with electrons, the meson is usually captured in a circular orbit (about one 210th the size of a corresponding electron Bohr orbit). The meson then continues to lose energy by ejecting electrons from the atom (similar to the Auger effect) until the principle quantum number is of the order of the square root of Z. At

this point, the diminishing Auger transition-probability is overtaken by the increasing probability of radiative transitions and meson begins to emit hard x-rays, finally reaching 2p and 1s orbitals in a total time of 10^{-15} to 10^{-13} seconds. It remains in this orbit until it decays or is absorbed by the nucleus in a time of 10^{-6} or 10^{-7} seconds.

Electron Scattering

By utilizing phase shift calculations and a model of nuclear charge distribution, the radius of the nucleus can be determined very accurately from electron scattering experiments. Yennie, Ravenhall, and Willson[35] have used several models which seem to indicate that the smoothed uniform charge distribution is in the closest agreement with experiment. This result agrees with the work of Crawford and Schawlow mentioned earlier. Both methods seem to indicate a value of 1.2×10^{-13} cm for r_o.

Other methods for Determining r_o and Validity of Radii

The other methods available rely on an assumed knowledge of the nuclear forces. These results are larger, for the most part, than 1.2×10^{-13} but are still smaller (in general) than the previously used value of 1.4×10^{-13}. Williams[36] has discussed the validity of the various methods.

At present because of their accuracy and agreement, the μ mesic atom experiments and the electron scattering measurements seem to give the best value for r_o.

IV. C. Screening effects

So far, the shift has been considered only in terms of an ns electron. This is justifiable only in the absence of screening effects. The effect of screening an ns electron by a d electron or mutual screening by s^2 electrons has been treated by Kopfermann[3] and also by Crawford and Schawlaw.[21]

Thus far this paper has considered only the penetration by the valence electron of the shell core, and has regarded the closed shell electronic core of the atom as rigid. However, when the atom is ionized, the valence electron is removed and thus its screening effect on the electronic core is removed and the core electrons move in closer to the nucleus. Disregarding the normal mass effect, the measured value of the isotope shift differs from the expected shift associated with the ns electron by a factor $\delta T_{exp} = (1-\alpha)\delta T_{ms}$. Crawford and Schawlaw[21] have made a first order estimate of the value of α in Hg. They give $\alpha \leq .16$. This is calculated from the Hartree functions for Hg. Kopfermann[3] assumes that α is nearly zero for most heavy elements.

V. EXPERIMENTAL ARRANGEMENT

1. Chromium

Chromium has stable isotopes at M= 50,52,53 and 54. For these isotopes the isotope shift has not been studied extensively. Since Arroe[37] has done work on the chromium isotopes 52 and 53, (see Table I) this experiment was performed to supplement the data by including Cr^{50}. Natural chromium was used. The relative abundances of the naturally occurring isotopes are: Cr^{50}-4.5%, Cr^{52}-83.8%, Cr^{53}-9.4%, and Cr^{54}-2.3%. The isotope shifts, Cr^{50}-Cr^{52} and Cr^{52}-Cr^{53}, should be observable with the equipment to be described. The chromium lines that were investigated and their term values are given in table II.

2. Hollow Cathode Light Source

The hollow cathode discharge tube was originally developed by H. Schuler.[38] The discharge tube used in this experiment is a modified Schuler type developed by Austern, Mack, and Arroe.[39] It differs in several respects from the original Schuler tube.[40] The tube used in this case was manufactured by Radio Corporation of America for Dr. Arroe and its important features are shown in fig 4. The main portion of the tube is of soft glass with the anode and

TABLE I

Results of Arroe's work[36] on the isotope shift Cr^{53}-Cr^{52}

Term	Shift (in mK)
$d^4s^2\ {}^5D_4$-$d^5p\ {}^5P_3$	+42.9±1.0
$d^4s^2\ {}^5D_3$-$d^5p\ {}^5P_3$	41.0±0.8
$d^4s^2\ {}^5D_3$-$d^5p\ {}^5P_2$	40.3±2.0
$d^4s^2\ {}^5D_2$-$d^5p\ {}^5P_3$	40.0±2.0
$d^4s^2\ {}^5D_2$-$d^5p\ {}^5P_2$	40.0±2.0
$d^4s^2\ {}^5D_2$-$d^5p\ {}^5P_1$	39 ±3
$d^4s^2\ {}^5D_1$-$d^5p\ {}^5P_2$	41 ±2
$d^4s^2\ {}^5D_1$-$d^5p\ {}^5P_1$	41.0±0.8
$d^4s^2\ {}^5D_0$-$d^5p\ {}^5P_1$	41.3±1.0

TABLE II

Lines investigated and their term values[36]

Term Combination			Term value (in K)
$d^5(^6S)_5$	$^5S_2$ - $d^5(^6S)p$	$^5P_3$	19194.2
		$^5P_2$	19203.0
		$^5P_1$	19208.7
$d^5(^6S)$	$^5S_2$ - $d^4s(^6D)p$	$^7D_1$	19707.2
$d^4\ s^2$	$^5D_4$ -	$^5P_3$	18479.8
	$^5D_3$ -	$^5P_3$	18692.1
	$^5D_3$ -	$^5P_2$	18700.9
	$^5D_2$ - $d^5(^6S)p$	$^5P_3$	18859.9
	$^5D_2$ -	$^5P_2$	18868.7
	$^5D_2$ -	$^5P_1$	18874.4
	$^5D_1$ -	$^5P_2$	18985.4
	$^5D_1$ -	$^5P_1$	18991.1
	$^5D_0$ -	$^5P_1$	19051.1

cathode of covar. The dimensions of the tube are such as to give it an f-number of 3 which is required to match the optics of the spectrograph and will be discussed later. The power supply used in conjunction with the discharge tube was voltage regulated, the high voltage being applied through suitable stabilizing resistors. Most of the exposures were taken with the current through the tube in the range of 100 to 125 milliamperes and with a voltage drop of about 450 volts across the tube. The current density in the hollow cathode was about 160 ma/cm^2, a value which should not be exceeded because of the Stark effect.

The walls of the hollow cathode must be quite uniformly coated with chromium to give a good spectrum. This was accomplished by carefully pouring Cr_2O_3 powder through the gas inlet of the tube and adding enough distilled water to fill the hollow cathode. With the powder in suspension, the cathode was heated slowly. As the water evaporated, a thin layer of Cr_2O_3 was deposited on the wall of the cathode. This procedure had to be repeated several times during the course of the experiment.

The hollow cathode discharge tube is cooled by liquid air to reduce the Doppler width (see fig. 2). The Doppler

width of the lines depends upon the temperature according to the equation

$$\Delta\sigma = \sigma\,(7.1\times10^{-7})\sqrt{\frac{T}{M}}$$

where T is the temperature (°K) of the discharge and M is the mass number of the atom. The Doppler width is due to the random motions of the atoms of the gas. The individual atoms emit mono-chromatic light in the reference system moving with them, but if the atom is moving with a velocity $\vec{v}$ relative to an observer, the frequency to the observer appears shifted by an amount $\nu_0\,\vec{v}/c$ compared with the frequency ν_0 of the source at rest.

3. The Gas Filling System

Two kinds of rare gas supply systems are readily adaptable to this type of experiment. One is a system in which the gas is circulated through the system by means of a mercury diffusion pump. The other, which was used in this experiment is much less complicated, consisting only of a container for the rare gas and a charcoal trap through which the gas must pass to reach the discharge tube. The purpose of the charcoal trap is to remove any impurities that may be in the rare gas or that may have entered the system from the Cr_2O_3.

The charcoal trap is cooled by liquid air to improve its efficiency. Two valves separated by a short length of glass tubing are inserted between the gas container and the charcoal trap permitting the addition of small amounts of gas to the discharge tube. The rare gas container was made from a Pyrex flask with a capacity of about 1 liter. In this experiment, it was filled with helium to a pressure of about 750 mm Hg.

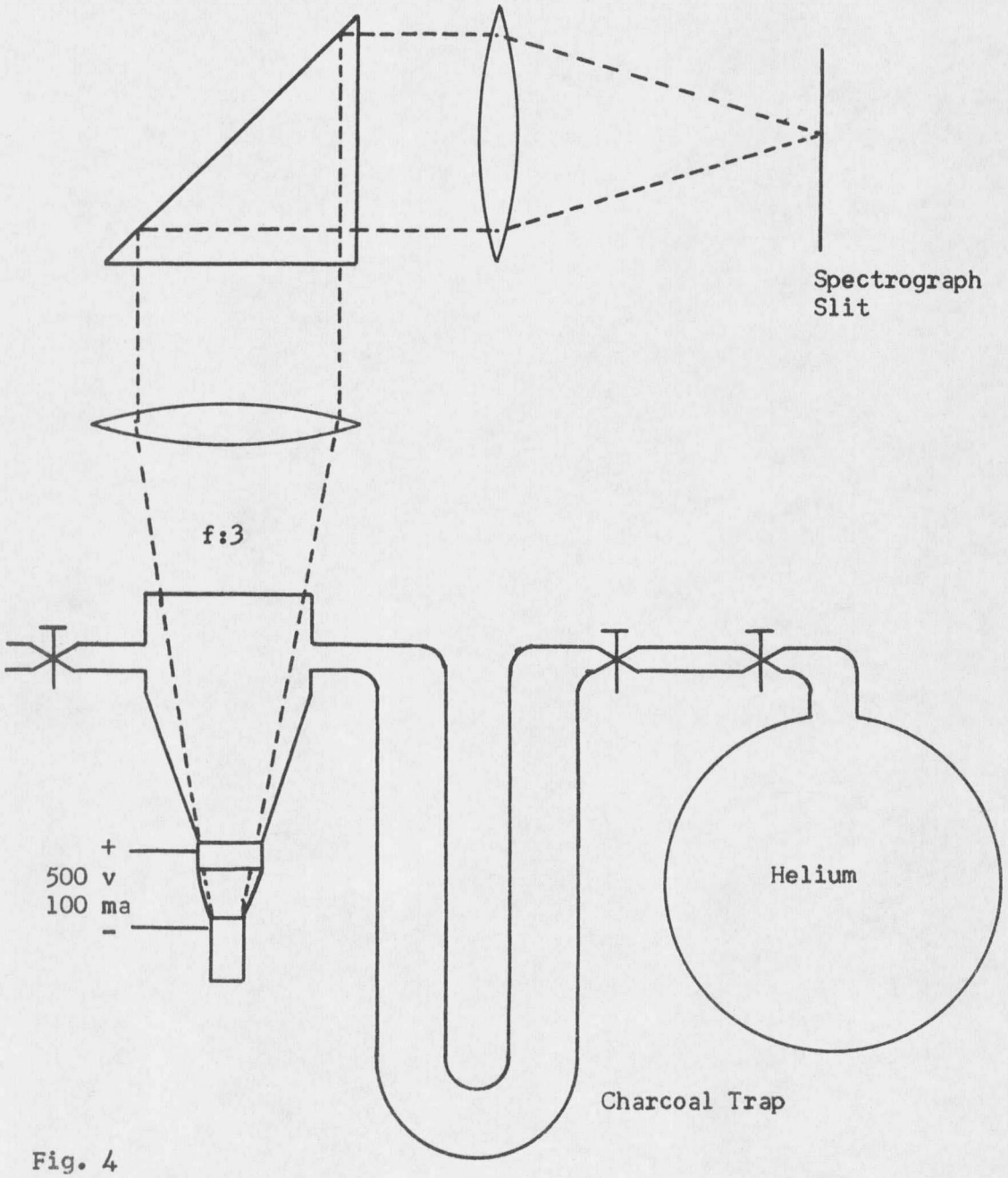

Fig. 4

Hollow Cathode and Simple Gas Filling System

4. The Fabry-Perot Interferometer

The principles of the Fabry-Perot interferometer are covered in most intermediate optics textbooks. However, a brief review of the fringe pattern will be given here preliminary to a discussion of the data reduction and the effect of varying pressure on the interferometric pattern.

A schematic diagram of the Fabry-Perot interferometer is shown in fig. 5a. The conditions for maxima are $2d\cos\theta = m\lambda$, $m = 0, 1, 2 \cdots$. The fringes are concentric circles with the origin as the center. Each circle corresponds to a given value of θ . A ring disappears each time d is decreased by $\lambda/2$. The rings nearest the center have the largest values of n. The intensity of the finges is given by

$$I = I_{max} \Big/ \left[1 + \frac{4r^2}{(1-r^2)^2} \sin^2 (\delta/2) \right]$$

where r is the reflectivity of the plates and δ is the phase difference, the refecting power $\rho = r^2$, and δ is determined from

$$\delta = \frac{4\pi d \cos\theta}{\lambda}$$

The half-intensity width of the instrument, $\Delta\sigma$, is given

$$\Delta\sigma = \frac{1-r}{2\pi d\sqrt{r}} \quad .$$

(See fig. 2). From the conditions on the maxima, it is seen that the distance between fringes is $\Delta\sigma = 1/2d$. Since a shift of about 80-40 mK was expected in this experiment, d was required to be about 15-20 mm.

The change of the pressure of the air between the Fabry-Perot flats can cause a shift in the spectral lines. This 'pressure shift' may be calculated from the Lorenz-Lorentz law:

$$\frac{n^2-1}{n^2+2} \cdot \frac{1}{\rho} = \text{CONSTANT}$$

where ρ is the density of the air, and n is the index of refraction of the air. This law may be rewritten as

$$\frac{n'-1}{n''-1} = \frac{p'}{p''} \quad \text{or} \quad \frac{\Delta n}{n-1} = \frac{\Delta p}{p} \quad .$$

Using

$$\Delta p = 1 \text{ cm Hg}, \quad p = 760 \text{ mm Hg}, \quad n = 1.00025,$$

one obtains $\Delta n \approx 3.0 \times 10^{-6}$. However, Δn may be rewritten in terms of $\Delta\sigma$ with $2d\sigma\,\Delta n = \Delta\sigma$ therefore, for

$\sigma = 20{,}000\,K$, $\Delta\sigma \approx 60\,mK$. Thus, on long exposures a change in atmospheric pressure of 1 cm could cause a significant broadening of the fringes.

Two different Fabry-Perot interferometers were used. The frame of one was constructed of solid invar stock and the frame of the other of solid brass stock. The spacers were corrected for uniform width by checking for flatness with two silvered glass plates. The spacers were made of an invar alloy that has a low coefficient of expansion at room temperature. The quartz flats were adjusted on the frame in the usual manner. Fig. 5b shows the details of the frame.

The quartz flats were silvered in an evaporation unit such as that described by Tolansky;[40] this is a brass tube 85 cm long and 10 cm in diameter. The quartz plates are mounted near the ends of the tube and silver is placed on a filament at the center of the tube. When the tube is evacuated, the filament is heated by an electric current and the plates are silvered very evenly.

Fig. 5

Fabry - Perot Interferometer

a.

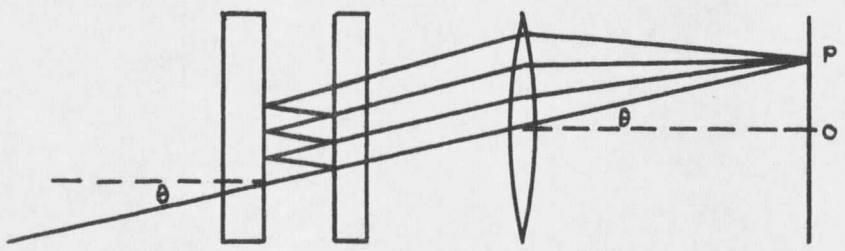

b.

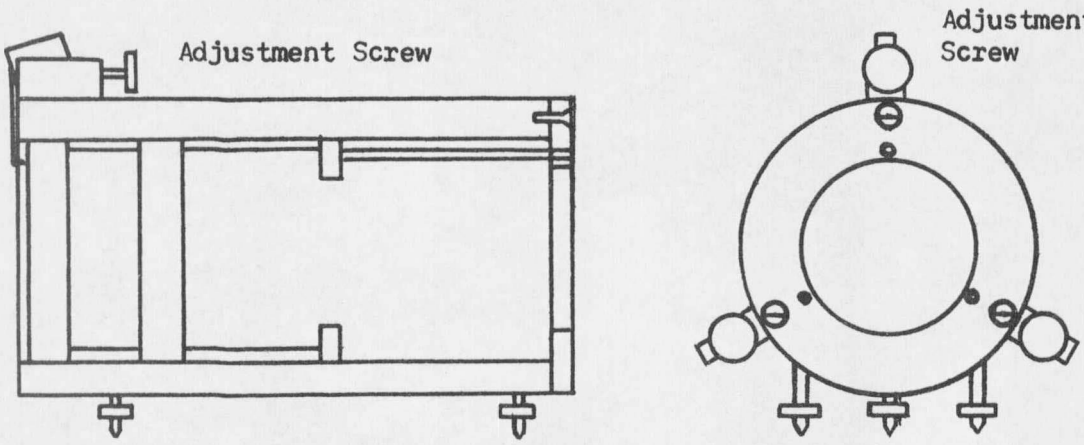

5. Spectrograph

A three prism Steinheil-Streander spectrograph was available for this experiment. The spectrograph was focused by means of the 5875, 5015, and 4713 Å helium lines and the dispersion curve was measured using known helium and chromium lines. With this curve, the lines on the photographic plates could be readily identified.

The collimator of the spectrograph has dimensions giving an f-number of 9. A magnification of about 3 was required to utilize the entire height of the photographic plate. Thus the light source had to be f/3.

6. Film and Exposures[42]

A spectroscopic plate of high sensitivity in the green wavelengths was desired for this experiment. The plate chosen was Kodak 103a-G. This plate has strong sensitivity throughout the blue and green regions with a maximum at about 5550 Å . It has a sharp cut-off just beyond 5700 Å on the long wavelength side. Consequently, this plate has very good green sensitivity without appreciable red sensitivity.

Due to the small relative percentage of some of the isotopes in natural chromium which were studied, long exposures had to be taken. For example, if the Cr^{52} components

were just observable, an increase in exposure of about 400 times would be necessary to just observe the Cr^{50} components.

Exposures of about 5 hours duration were used to obtain the data reported here. In all, 27 different exposures were taken, including exposure times up to 12 hours in length. Some of the plates were not suitable for reading of data due to maladjustment of the interferometer, effects of incorrect temperature of the D19 developer, and effects of the pressure shift.

7. Data Reduction

The maxima for the Fabry-Perot interferometer are given by

$$2d \cos\theta = n\lambda$$

A ray of light entering the interferometer at an angle θ enters the spectrograph telescope at the same angle. The ray is focussed at a distance proportional to $\tan\theta$ from the center of the telescope and since n is very large, θ is very small and one may set $\tan\theta \approx \theta$ and $\cos\theta \approx 1 - \theta^2/2$. Thus the diameter of a fringe obeys the relationship

$$x^2 = (1 - \cos\theta)\, C$$

where C is a proportionality constant. The square of the fringe diameter is

$$x_m^2 = \left(1 - \frac{m\lambda}{2d}\right) C \quad .$$

But n is a large integer and d is a relatively small number, therefore,

$$\frac{m\lambda}{2d} >> 1 \quad .$$

Thus the difference of squares of fringe diameters is given by

$$x_m^2 - x_m'^2 = \frac{Cm}{2d}(\lambda - \lambda') \quad .$$

Since

$$x^2 = (1 - \cos\theta)\, C$$

is the fringe diameter squared, and $m\lambda = 2d\cos\theta$ then

$$x_m^2 - x_{m+1}^2 = \frac{C\lambda}{2d}$$

From this expression,

$$\frac{C}{2d} = \frac{x_m^2 - x_{m+1}^2}{\lambda} \quad ,$$

and from the equation for the difference of squares of fringe diameters, $x_m^2 - x_m'^2$, we obtain the result

$$m(\lambda' - \lambda) = \frac{\lambda(x_m^2 - x_m'^2)}{x_m^2 - x_{m+1}^2}$$

Again, by means of the condition for maxima, and with θ small, the final result is

$$\frac{x_m^2 - x_m'^2}{x_m^2 - x_{m+1}^2} = \frac{\lambda - \lambda'}{\lambda^2}$$

where

$$\frac{\lambda - \lambda'}{\lambda^2}$$

is the wave number difference, $\Delta\sigma$.

In practice, the fringe positions for a single line are read on a microcomparator. These positions are recorded as one reads from the edge of the fringe pattern to the center of the pattern and then to the opposite edge. Thus, the diameter of a fringe is found. An array of numbers, from which the isotope shift may easily be calculated, is set up in the following manner:

$$\begin{array}{cccc} x_m'^2 & x_{m+1}'^2 & x_{m+2}'^2 & \cdots \\ x_m''^2 & x_{m+1}''^2 & x_{m+2}''^2 & \cdots \\ \vdots & \vdots & \vdots & \\ \vdots & \vdots & \vdots & \\ \vdots & \vdots & \vdots & \end{array}$$

Let D be the average of all the $(x'^2_m - x'^2_{m+1})$, $(x''^2_m - x''^2_{m+1})$, ... Then the shift between components is given by

$$\frac{1}{mD}\left(\frac{1}{2d}\right)\sum_m (x'^2_m - x''^2_m) = \Delta\sigma$$

where d is the interferometer spacing.

For the measurements reported here, all readings on the photographic plates were taken with a Hilger microcomparator which is capable of reading positions to 0.001 mm.

VI. CONCLUSION

The results of the data reduction are listed in table III. The volume effect was included as well as the normal mass effect. The residual shift was obtained by subtracting the normal mass effect and by adding the volume effect. The volume effect was calculated from the formula derived by Rosenthal & Breit for a uniform charge distribution within the nucleus. That is:

$$\Delta\delta W = \frac{4T^{3/2}}{z_0 R^{1/2}} \left(1 - \frac{d\sigma}{dm}\right) \frac{1+\rho}{[\Gamma(2\rho+1)]^2} y_0^{2\rho} \frac{\Delta y_0}{y_0} \frac{3}{(2\rho+1)(2\rho+3)}$$

with

$$\rho = \sqrt{1 - \alpha^2 z^2} = 0.925$$

$$\alpha = \frac{2\pi e^2}{hc} = 1/137.03$$

$$y_0 = \frac{2zr}{a_0}$$

$$z = 24$$
$$z_0 = 1$$
$$a_0 = 0.529 \times 10^{-8} \text{ cm}$$
$$r = 1.2 \times 10^{-13} A^{1/3} \text{ cm}$$

Due to the complexity of the spectra, $\Delta\sigma/\Delta m$ was calculated rather than $d\sigma/dm$. This ratio of differences was found to vary from zero by not more than ± 0.04. Thus to a good approximation one can say $\Delta\sigma/\Delta m = 0$. With these values, the volume effect becomes

$$\Delta\delta W = T^{3/2}\ 1.50 \times 10^{-9} .$$

For example, at

$$T = 20{,}000\ K\ , \quad \Delta\delta W = 4.24\ mk .$$

The normal mass effect shift was calculated as was indicated in part II. That is:

$$\Delta\sigma = \frac{\sigma}{1836.12}\left(\frac{M_2 - M_1}{M_2 M_1}\right) .$$

A. Comparison of Results

The shift reported here is that from Cr^{52}-Cr^{50}. However, the shift Cr^{53}-Cr^{52} could also be read. The values obtained for this shift are not reported since Arroe's work with separated isotopes afforded much better accuracy. The shift Cr^{53}-Cr^{52} was found to be 42 ± 6 mk. This is in good agreement with the earlier work of Arroe (see table I).

The uncertainty shown in table III is the average of all rms deviations from the mean value for all lines read.

The uncertainty given in table I is the largest deviation from the mean value of all plates read.[38]

At the present state of the theory, the residual shift

indicated in table III can probably be attributed only to the specific mass effect as this is the only remaining effect that can account for such a large observed shift.

Due to the extreme complexity of the calculation of the specific mass effect shift, there is no comparison of theoretical and experimental results.

TABLE III

Results for the isotope shift $Cr^{52} - Cr^{50}$

Term Combination	Term Value	Volume Shift (in mK)	Normal Mass Shift (in mK)
$^5D_4 - {}^5P_3$	18484.9	4	7.7
$^5D_1 - {}^5P_1$	18996.2	4	7.7

Term Combination	Experimental Shift (in mK)	Residual Shift (in mK)
$^5D_4 - {}^5P_3$	85±5	81±5
$^5D_1 - {}^5P_1$	84±5	81±5

LITERATURE CITED

1. Meggers, W. F., J. Opt. Soc. Am. 36, 431, (1946)

2. Michelson, A., Phil. Mag. 31, 388, (1891)

3. Kopfermann, H., Nuclear Moments, (Academic Press, New York, N. Y., 1958)

4. Pauli, W., Naturwissenschaften, 12, 741, (1924)

5. White, H., Introduction to Atomic Spectra, (McGraw-Hill Book Co. Inc., New York, N. Y., 1934), chpt. 2

6. Back, E. and Goudsmit, S., Z. Physik 43, 321, (1927)

7. Mack, J. and Arroe, H., Ann. Rev. Nuclear Sci. 6, 177, (1956)

8. Panofsky, W. and Phillips, M., Classical Electricity and Magnetism, (Addison-Wesley Pub. Co., Reading, Mass., 1955), p. 171

9. Landau, L. and Lifschitz, E., Classical Theory of Fields, (Addison-Wesley Pub. Co., Reading, Mass., 1951) p. 107

10. Casimir, H., Teylors Tweede Genootshap 11, (1936)

11. Kuhn, H. G., Atomic Spectra, (Academic Press, New York, N. Y., 1962), p. 347

12. Hughes, D. J. and Eckart, C., Phys Rev. 36, 694, (1930)

13. Bartlett, J. H. Jr. and Gibbons, J. J. Jr., Phys. Rev. 44, 459, (1933)

14. Vinti, J. P., Phys. Rev. 56, 1120, (1939)

15. Rosenthal, J. and Breit, G., Phys. Rev. 41, 495, (1932)

16. Racah, G., Nature 129, 723, (1932)

17. Goudsmit, S., The Structure of Line Spectra, (McGraw-Hill Book Co. Inc., New York, N. Y., 1930) p. 202

18. Goudsmit, S., Phys. Rev. 43, 636, (1933)

19. Breit, G., Phys. Rev. 42, 348, (1932)

20. Fermi, E. and Segre, E., Z. Physik 82, 729, (1933)

21. Crawford, M. F. and Schawlow, A. L., Phys. Rev. 76, 9, 1310, (1947)

22. Bethe, H., Elementary Nuclear Theory, (John Wiley and Sons, Co., New York, N. Y., 1943), p. 9

23. Brix, P. and Kopfermann, H., Z. Physik 126, 344, (1949)

24. Humbach, W., Z. Physik 133, 589, (1952)

25. Halliday, D., Introductory Nuclear Physics, (J. Wiley and Sons Co., 1955), p. 272

26. Eisberg, R., Fundamentals of Modern Physics, (J. Wiley and Sons Co., New York, N. Y., 1961) p. 592 and p. 608

27. Wilets, L., Hill, D., and Ford, K., Phys. Rev. 91, 6, 1487, (1953)

28. Goeppert-Mayer, M. and Jensen, H., Elementary Theory of Nuclear Shell Structure, (J. Wiley and Sons Co., New York, N. Y., 1955), chpt. 2

29. Bohr, A. and Mottelson, B. R., Dan. Mat. Fys. Medd. 27, (1953), No. 16

30. Elasser, W., J. phys. radium 4, 549, (1933)

31. Rainwater, L. J., Phys. Rev. 79, 432, (1951)

32. Scott, J., "The Radius of the Nucleus", Progress in Nuclear Physics, 5, (1956)

33. Wheeler, J. A., Revs. Mod. Phys. 21, 133, (1953)

34. Fitch, V. and Rainwater, J., Phys. Rev. 101, 1131, (1956)

35. Yennie, D. R., Raventhall, D., and Willson, Phys. Rev. 95, 500, (1954)

36. Williams, R. W., Phys. Re. 98, 1387, (1955)

37. Arroe, H., Studies over Spektralliniers Struktur, (Copenhagen, 1951)

38. Schuler, H., Z. Physik 59, 150, (1930)

39. Arroe, H., private communication

40. Arroe, H. and Mack, J. E., J. Opt. Soc. Am. 40, 6, 386, (1950)

41. Tolansky, High Resolution Spectroscopy, (Methuen, New York, 1947)

42. Kodak Photographic Plates for Scientific and Technical Use, (Eastman-Kodak Co., Rochester 4, N. Y.)

43. Candler. C., Modern Interferometers, (Hilger and Watts Ltd., Hilger Division, Glasgow, Scotland, 1951) p. 307